

Geological Society of America Bulletin

Coeval hindward- and forward-imbricating thrusting in the south-central Pyrenees, Spain: Timing and rates of shortening and deposition

DOUGLAS W. BURBANK, JAUME VERGÉS, J. ANTON MUNOZ and PETER BENTHAM

Geological Society of America Bulletin 1992;104, no. 1;3-17
doi: 10.1130/0016-7606(1992)104<0003:CHAFIT>2.3.CO;2

Email alerting services click www.gsapubs.org/cgi/alerts to receive free e-mail alerts when new articles cite this article

Subscribe click www.gsapubs.org/subscriptions/ to subscribe to Geological Society of America Bulletin

Permission request click <http://www.geosociety.org/pubs/copyrt.htm#gsa> to contact GSA

Copyright not claimed on content prepared wholly by U.S. government employees within scope of their employment. Individual scientists are hereby granted permission, without fees or further requests to GSA, to use a single figure, a single table, and/or a brief paragraph of text in subsequent works and to make unlimited copies of items in GSA's journals for noncommercial use in classrooms to further education and science. This file may not be posted to any Web site, but authors may post the abstracts only of their articles on their own or their organization's Web site providing the posting includes a reference to the article's full citation. GSA provides this and other forums for the presentation of diverse opinions and positions by scientists worldwide, regardless of their race, citizenship, gender, religion, or political viewpoint. Opinions presented in this publication do not reflect official positions of the Society.

Notes



Coeval hindward- and forward-imbricating thrusting in the south-central Pyrenees, Spain: Timing and rates of shortening and deposition

DOUGLAS W. BURBANK *Department of Geological Sciences, University of Southern California, Los Angeles, California 90089*

JAUME VERGÉS *Servei Geològic de Catalunya, Avenida Paral·lel 71, 08015 Barcelona, Spain*

J. ANTON MUÑOZ *Departament de Geologia Dinàmica, Universitat de Barcelona, Zona Universitaria de Pedralbes, 08071 Barcelona, Spain*

PETER BENTHAM *Department of Geological Sciences, University of Southern California, Los Angeles, California 90089*

ABSTRACT

Clear demonstrations of detailed sequences of thrust development are rare, particularly with respect to hindward-imbricating successions. Similarly, well-constrained chronologies of the timing of multiple thrust motions and associated rates of shortening are also uncommon. Along the eastern oblique ramp of the South-Central Unit (SCU) of the Pyrenees, well-exposed structural geometries and crosscutting stratigraphic packages unambiguously illustrate a sequence of break-back thrusts that developed synchronously with the growth of an adjacent duplex. The break-back sequence includes both the Sierras Marginales and Montsec thrusts: structures defining two of the major east-west partitions within the SCU. Balanced, sequentially restored structural cross sections indicate that a minimum of 7.5 km of shortening occurred within the imbricate stack. An additional 9 km of contraction was accommodated by the duplex, prior to translation of the duplex and imbricate stack to the south along a detachment within upper Eocene evaporites. Magnetic polarity stratigraphies have been used to calibrate these late Eocene to Oligocene episodes of deformation. These temporal data indicate that Sierras Marginales thrusting began in the study area ~39.8 Ma and that the Montsec thrust ceased movement ~36.2 Ma, yielding a mean rate of shortening of 2.1 mm/yr. Coeval shortening within the duplex was ~2.5 mm/yr, and subsequent translation across the footwall ramp occurred at ~2.5–4 mm/yr. Despite the partitioning of shortening into distinctively different styles of deformation, the mean rate of contraction remained steady over ~4 m.y. These new chronologies indicate that the locus of large-scale thrusting did not progress systematically toward the

foreland, but shifted episodically within the SCU, such that, during the late Eocene shortening, the Sierras Marginales thrust was active both prior to and south of the Montsec thrust.

INTRODUCTION

As recently proposed models for the evolution of thrust wedges (for example, Davis and others, 1983) are tested against geological data, two problems repeatedly emerge. First, it is frequently difficult to demonstrate the actual sequence of thrust propagation, that is, whether it occurred as a series of piggyback thrusts propagating toward the foreland, break-back thrusts propagating toward the hinterland, or some combination of the two. Piggyback thrusting is widely accepted as the typical style of deformation in fold-and-thrust belts (Bally and others, 1966; Boyer and Elliott, 1982). Break-back thrusting, however, has recently been documented (Elliott and others, 1985; Martínez and others, 1988) and is, in fact, predicted by the mechanical thrust-wedge models (Davis and others, 1983; Platt, 1988). Second, even when the sequence of thrusting can be reliably reconstructed, the precise timing and duration of thrusting events are difficult to define. Frequently, several tectonic events will fall below the resolution of any known biostratigraphic limits, and, particularly in terrestrial sequences, such faunal data may be sparse.

The sequence of thrust propagation often can be unambiguously defined only by the relationships between thrusts and synorogenic sediments (for example, Martínez and others, 1988; Vergés and Muñoz, 1990). Such relationships are usually observed solely in the external portions of fold-and-thrust belts, where the absence of extensive uplift and associated deep erosion has preserved them. The problem of defining the

sequence of thrusting events can be addressed directly when crosscutting structural relationships are observable and, more specifically, when successive sedimentary aprons related to the emplacement of individual thrust sheets can be mapped. In addition, if these synorogenic sediments can be precisely dated (for example, Burbank and Reynolds, 1988; Jordan and others, 1988) and balanced cross sections can be constructed, then the problems of timing and rates of thrust development can also be assessed.

The southern Pyrenees provide an opportunity to apply the combined approaches of detailed mapping of thrusts and related synorogenic sediments with high-resolution dating techniques. Unlike many other youthful collisional mountain ranges, only moderate uplift has occurred adjacent to the external thrusts within the foreland. Limited erosion has exposed many of the thrusts, while also preserving clear syntectonic depositional relationships. Fine-grained sediments are present throughout much of the synorogenic succession and facilitate the successful application of magnetic polarity stratigraphy as a means to develop better temporal constraints.

In this study, we focus upon the boundary between the Ebro foreland basin and the South Central Unit (Séguret, 1972), a trapezoidally shaped thrust sheet involving Mesozoic to early Tertiary cover strata and extending ~90 km in an east-west direction and ~60 km in a north-south direction (Figs. 1 and 2). The recently published ECORS deep-seismic reflection profile traverses the eastern segment of the SCU (ECORS Pyrenees team, 1988; Roure and others, 1989; Muñoz, 1991). This seismic line reveals that, along this transect, the "Axial Zone" of the Pyrenees consists of a south-directed, crustal-scale duplex with an antiformal geometry that developed through piggyback thrusting. Although south- and north-directed imbricate thrust systems flank the Axial Zone, the majority

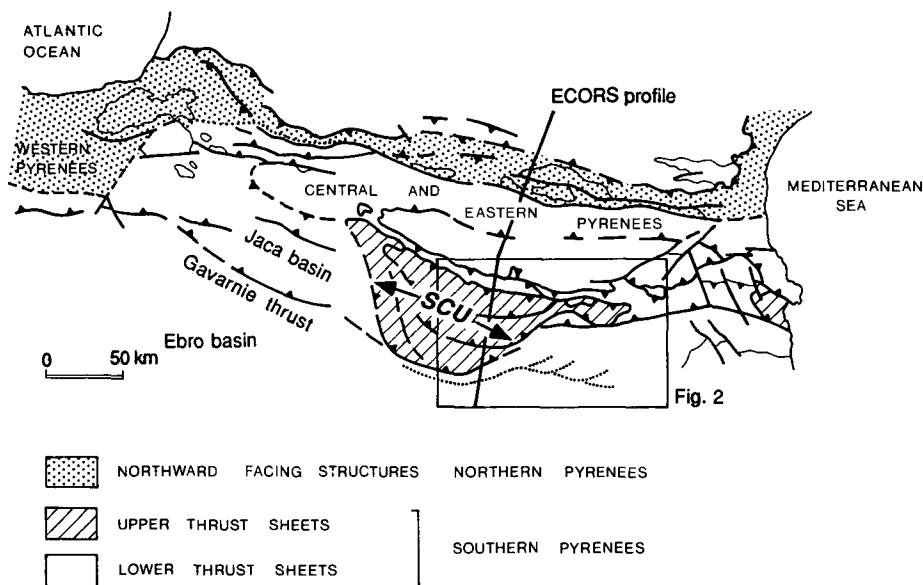


Figure 1. Generalized geologic map of the Pyrenees indicating major structural units. Dotted lines indicate the positions of buried thrusts and major anticlines in the Ebro basin. Box indicates the location of Figure 2.

of shortening is accommodated by the South Pyrenean thrust system. As the large-scale and deep-structural relationships are clarified by these new seismic data, it becomes increasingly useful to constrain more precisely the ages of deformation along this traverse in order to reconstruct the tectonic evolution of this region more reliably. We describe here an integrated stratigraphic, structural, and chronologic study of the northern portion of the eastern termination of the SCU, where we can define coeval break-back and piggyback thrust sequences, determine the magnitude of shortening on several thrusts, and document the ages and rates of thrust emplacement and synorogenic sediment accumulation.

GEOLOGIC SETTING

Structural Data

The SCU is bounded in the west by a set of anticlines and thrusts which separate it from the Gavarnie thrust sheet and in the east by the

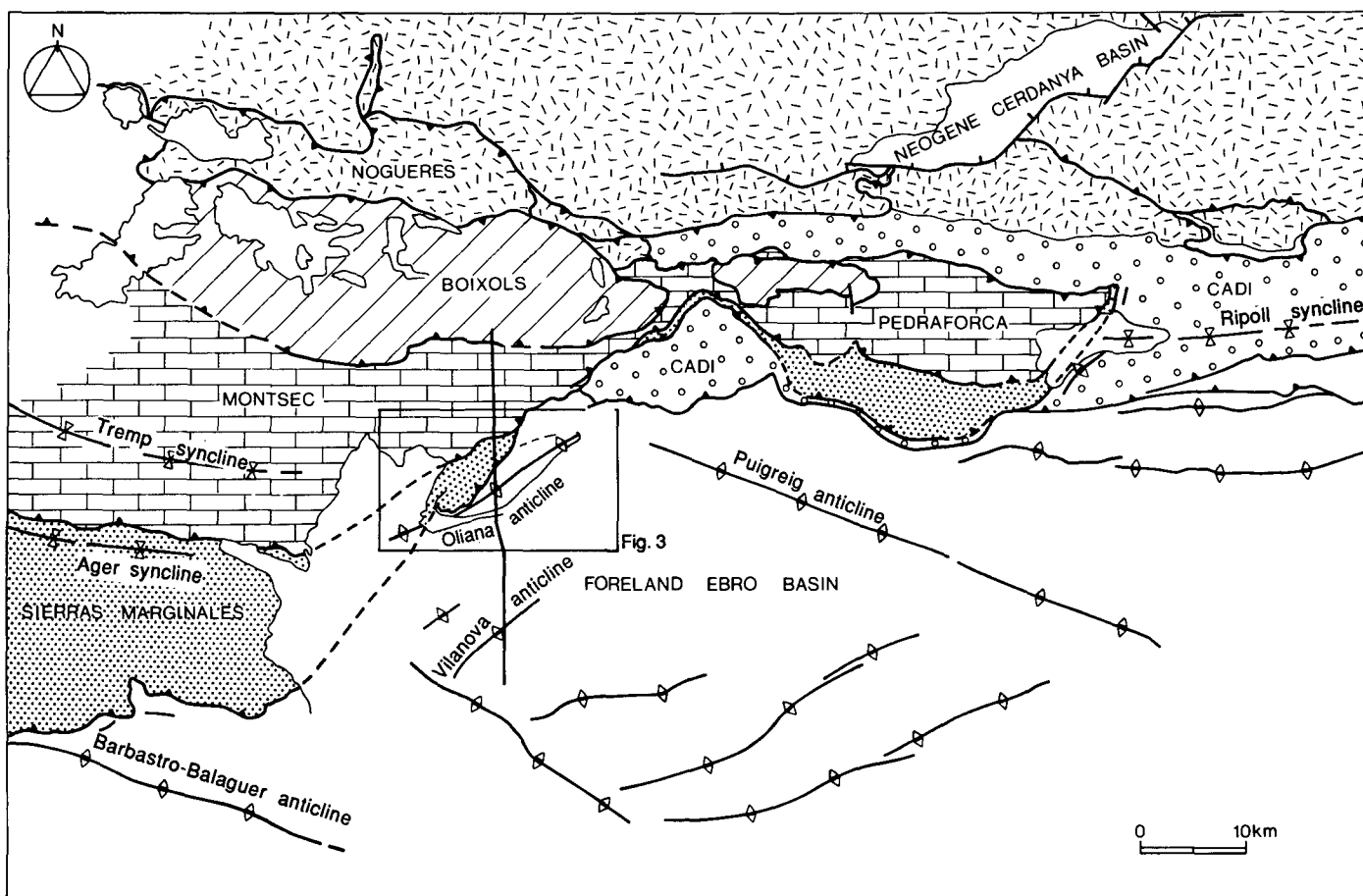


Figure 2. Simplified geologic map of the eastern South-Central Unit and the adjacent Pedraforca Unit showing the structural partitioning of each region, including the Boixols, Montsec, and Sierras Marginales thrust sheets in the SCU and the structurally equivalent units in the Pedraforca area. Box indicates the location of Figure 3 near the branching point of the Sierras Marginales and Montsec thrusts. The location of the structural cross section (Fig. 4) from the Boixols thrust to the Ebro foreland basin is shown by the approximately north-south line.

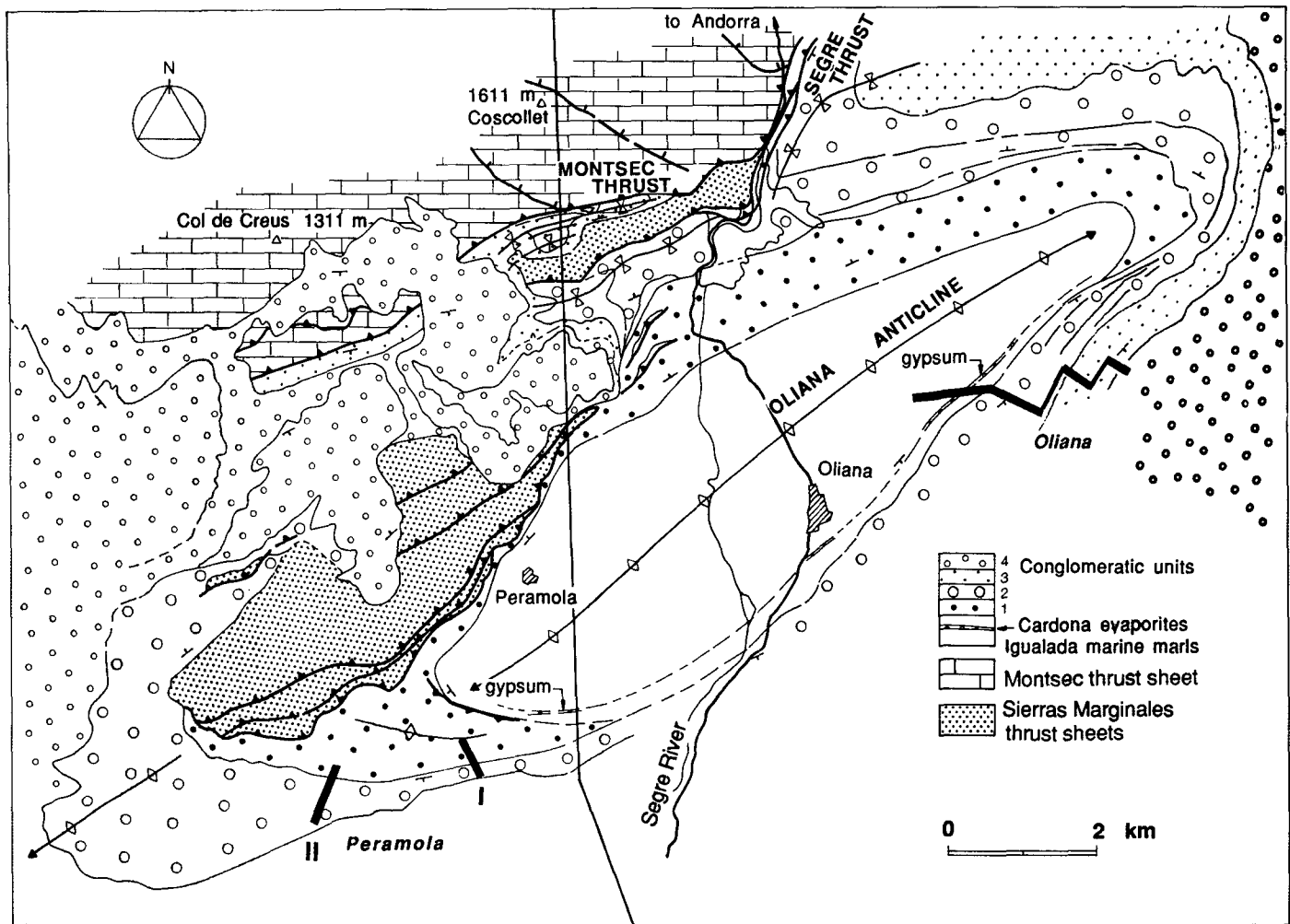


Figure 3. Geologic map showing major thrusts and stratigraphic units within the Oliana area along the eastern lateral ramp of the SCU. Conglomerate packages 1–4 are directly related to intervals of thrusting and show that the Sierra Marginales thrusts and the Montsec thrust formed in a break-back sequence. The gypsiferous strata on the map correspond to the Cardona evaporite. The locations of the magnetostratigraphic sections (Oliana and Peramola I and II) and the structural cross section are indicated.

Segre thrust, which separates the SCU from the Cadi thrust sheet (Figs. 1, 2, and 3). To the south and southeast, the SCU is bounded by the deformed Ebro foreland basin, whereas its northern limit is defined by the Noguera thrust sheets, which comprise both cover and basement rocks of the Axial Zone of the Pyrenees (Fig. 2).

Three major thrust sheets can be delineated within the SCU. From the north to south, these are the Boixols, Montsec, and Sierras Marginales thrust sheets. Farther south in the northern Ebro basin lie additional foreland folds and thrusts (Vergés and others, 1991). Deformation along the Boixols thrust occurred in late Maastrichtian time (Simó, 1985). An initial phase of movement of the Montsec thrust within the SCU affected the Ager syncline (Fig. 2) in the early Eocene (Mutti and others, 1985). In the western SCU, structural, stratigraphic, and magnetic data indicate that initial motion on the Montsec

thrust terminated by 54 Ma (Powers, 1989). Deformation within the Sierras Marginales (Fig. 2) along the southern border of the SCU is loosely constrained as ranging from middle Eocene to Oligocene (Puigdefàbregas and others, 1989).

In the northern portion of the eastern margin of the SCU, several thrusts can be observed which are lateral extensions of the Montsec and Sierras Marginales thrusts. These thrusts branch in a unique northeast-southwest-striking surface, the Segre thrust, which corresponds to the eastern oblique ramp of the SCU (Figs. 2 and 3). Oriented subparallel to the Segre thrust, the doubly plunging Oliana anticline is the northernmost structure along this traverse that does not involve pre-Tertiary strata. To the northwest of the Oliana anticline, geometrical relationships with synorogenic conglomerates demonstrate that the Mesozoic rocks of the SCU in the hanging wall of the Segre thrust are deformed by a

break-back imbricate stack. Details of the thrust geometry and sequencing are given by Vergés and Muñoz (1990). Seismic reflection profiles across the Oliana anticline clearly depict a zone of subhorizontal detachment at ~3 km beneath the crest of the structure. Well data indicate that this décollement corresponds to the upper Eocene Cardona evaporites and continues beneath the southern outcrops of the Montsec thrust sheet (Fig. 4).

Foreland Stratigraphic Series

The foreland stratigraphy commences with uppermost Cretaceous–lower Paleogene Garumnian red beds (Trempe Formation in the Pyrenean foreland basins) directly overlying the Hercynian basement rocks. Subsequently Ilerdian–Lutetian deposition on a carbonate platform (Alveolina limestone) was replaced by the

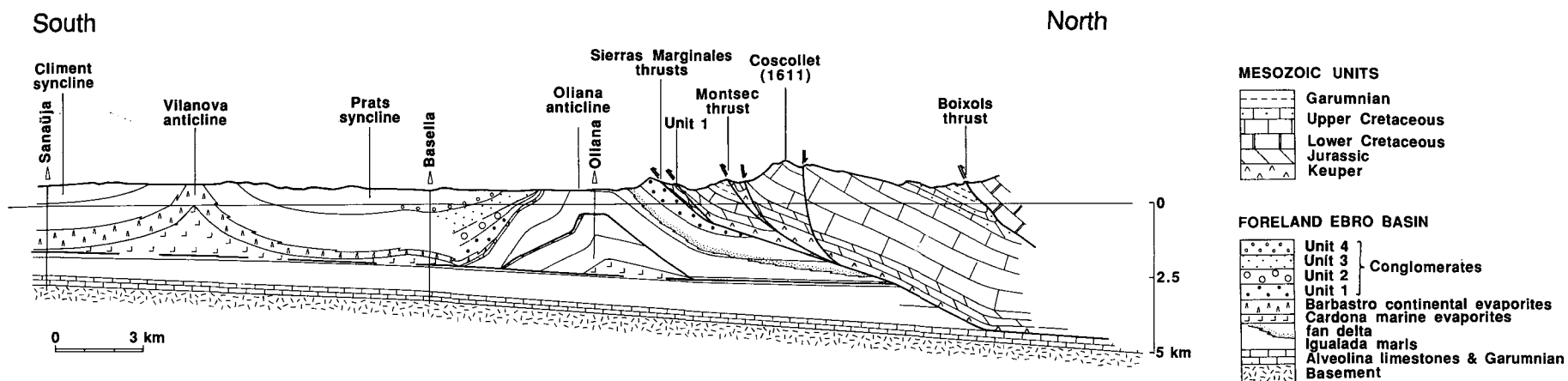


Figure 4A. Balanced cross section based on well (Oliana, Basella, and Sanaüja) and seismic data and on geological mapping (see location in Figs. 2 and 3). The pin-line for the three cross sections is the Sanaüja well. In between the Sierras Marginales and the Montsec thrusts, there is a thrust with conglomerate 1 in its footwall.

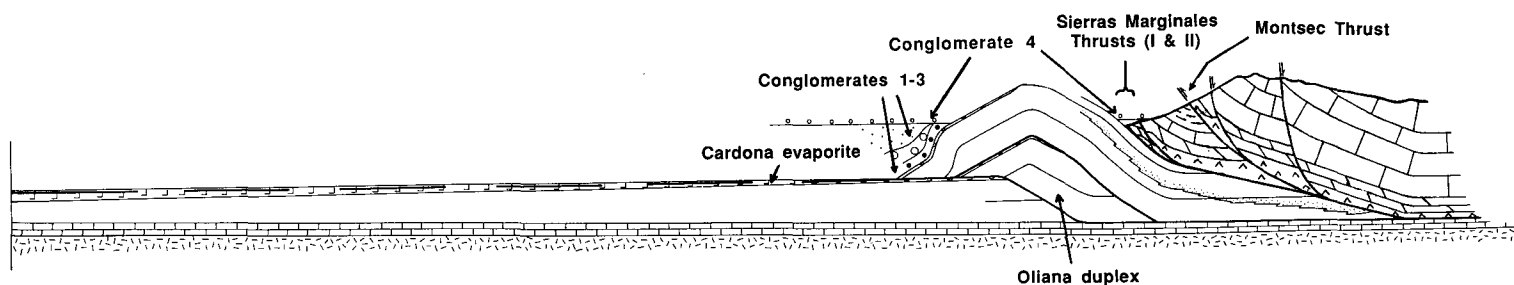


Figure 4B. Partially restored cross section at the time of initial deposition of conglomerate 4. The position of the Oliana duplex with respect to its translation across the footwall ramp and the height of the ramp itself are determined from altitudinal and deformational relationships presently visible along the base of conglomerate 4. Conglomerates 1-3 have been deformed by both the Oliana duplex and the imbricate thrusts, whereas conglomerate 4 remains undeformed.

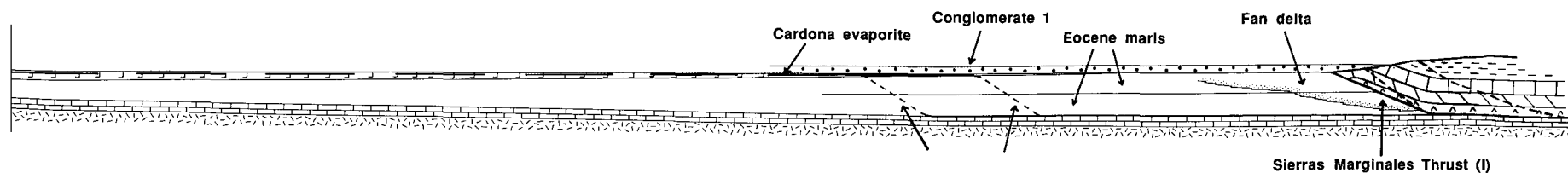


Figure 4C. Partially restored cross section at the time of deposition of conglomerate 1 which is clearly involved in the imbricate thrust system. Whereas the several future ramps through the marls are specified here, the cut-off for the Mesozoic strata of the thrust sheet is unknown. Future thrusts are marked by dashed lines.

Igualada marls. These marls crop out in the core of the Oliana anticline, attain a thickness of ~700 m in the Basella well (Fig. 4A), and have been micropaleontologically dated as late Bartonian–early Priabonian in age in the Oliana anticline (Caus, 1973). The upper portion of the marly sequence comprises lower Priabonian reefal limestone (Caus, 1973) in the southern limb of the anticline and fan-delta strata in the northern limb. They are succeeded by the lower Priabonian Cardona marine evaporites (gypsum and salt), representing the transition from marine to terrestrial conditions in this part of the Ebro basin (Sáez, 1987). These evaporites are overlain by >1,000 m of upper Eocene–lower Oligocene continental conglomerate (Fig. 4) which prograded generally to the south and which interfingers with evaporite (Barbastro continental gypsums) and lacustrine strata to the south and southeast.

METHODOLOGY

The study area was mapped at a scale of 1:25,000. Aerial photographic analysis and mapping permitted strike-line tracing of many of the sedimentary strata from positions adjacent to thrusts and folds in the west toward less deformed regions in the east (Fig. 3). Attention was focused on stratal packages that either overlay or were cut by thrusts, because they can most precisely define intervals of thrust motion. A balanced cross section, preserving bed lengths for the competent units and cross-sectional areas for the incompetent units, was constructed along a north-south transect. This orientation is subparallel to the transport direction inferred from the cartographic pattern of frontal and oblique thrust ramps in the eastern and central SCU. Although magnetic data from the western SCU reveal post-Paleogene clockwise rotations of the SCU (Powers, 1989; Dinarés and others, 1991), data from the eastern SCU exhibit no similar rotation. Consequently, it is reasonable to use the orientations of oblique and frontal structures as indicators of transport direction in this area. Due to the upper-crustal level of thrust emplacement, however, there is a paucity of reliable microstructural indicators that could confirm the inferred north-south transport direction which yields the minimum estimate of shortening.

Detailed mapping delineated four important detrital units (conglomerates 1–4) overlying the Igualada marls and the Cardona marine evaporites (Fig. 3). These units can be identified on both flanks of the Oliana anticline. On the northern margin, they are related directly with thrusts and consist of coarse-grained strata (breccia and conglomerate) interbedded with occasional siltstones. In this proximal area, the contacts between the units are generally angular

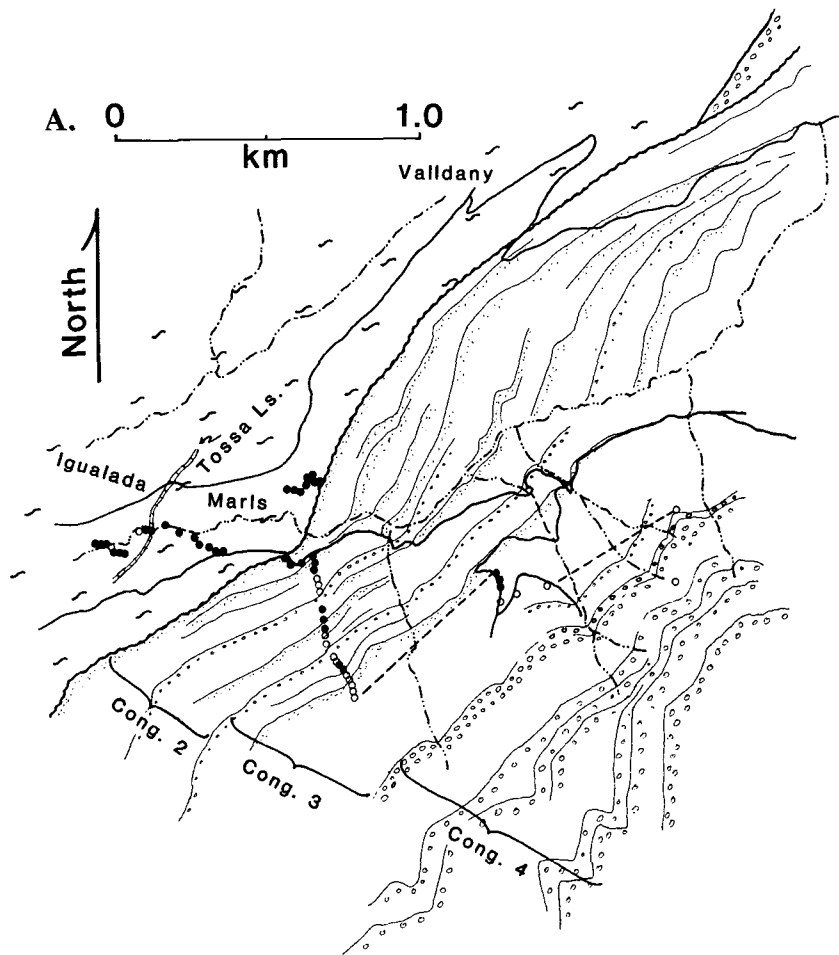


Figure 5A. Strike-line location map for the Oliana magnetic section. Site locations and polarity (normal = filled circles; reversed = open circles). See Figure 3 for location.

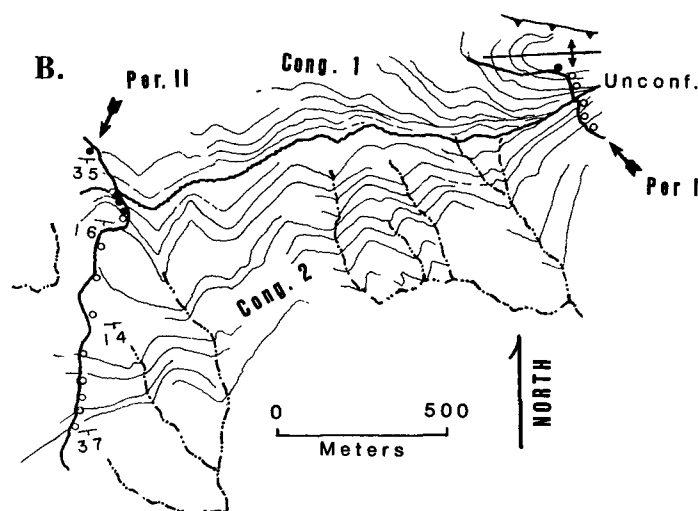


Figure 5B. Location map for the Peramola I and II magnetic sections. Note that the prominent unconformity between conglomerates 1 and 2 diminishes toward the west. See Figure 3 for location.

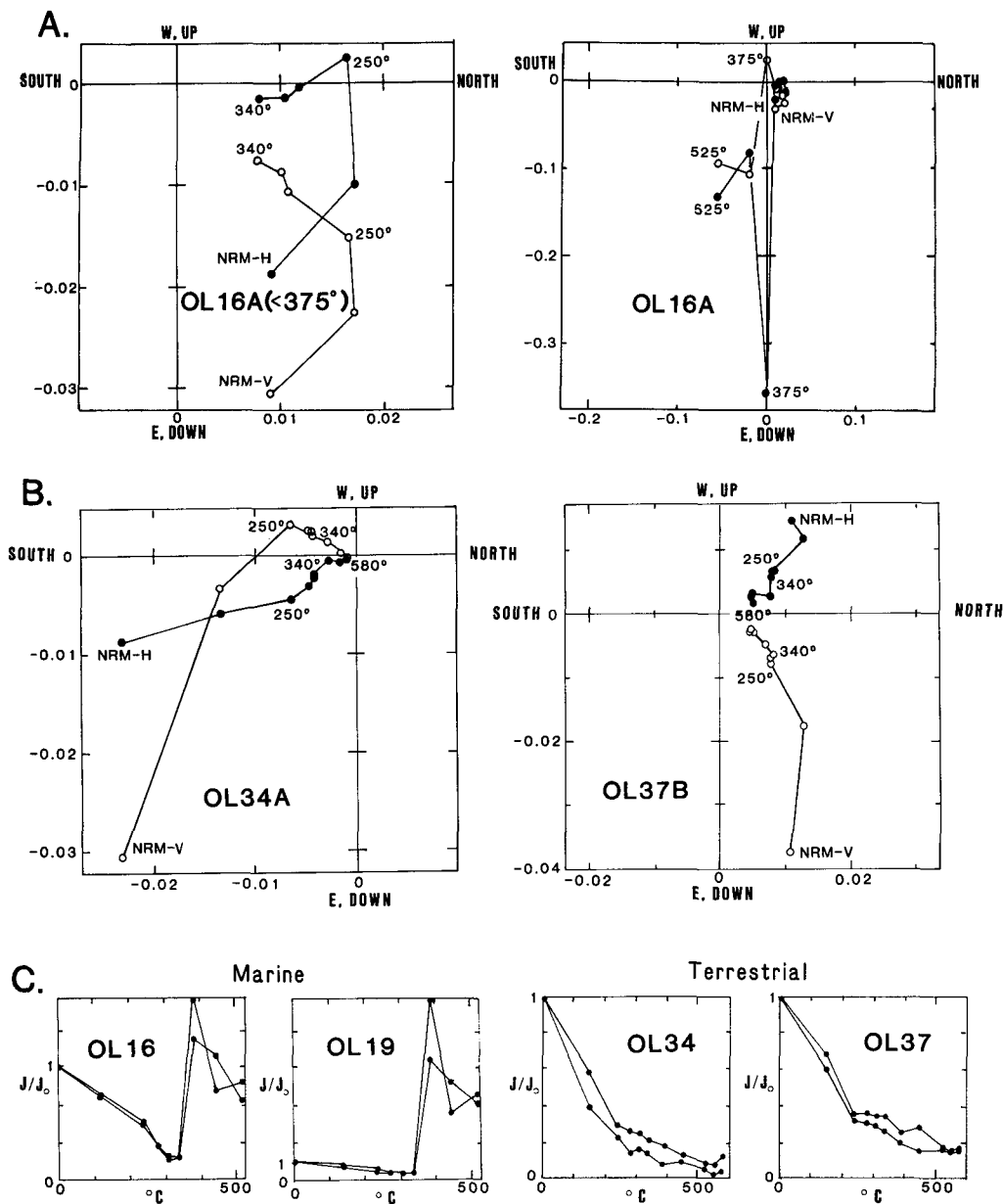


Figure 6A. Representative plots of thermal demagnetization curves for the Igalada marls at Oliana. The data show coherent, interpretable directions at temperatures <375 °C (left-hand plot), but they exhibit large intensity increases and unstable directions at temperatures >375 °C (right-hand plot).

Figure 6B. Representative plots of thermal demagnetization curves for two terrestrial siltstones at Oliana (OL34A: reversed polarity; OL37B: normal polarity), indicating rapid decreases in intensity at low temperatures and defining a characteristic remanence direction between 240 and 450 °C.

Figure 6C. Plots of changes in magnetic intensity during thermal demagnetization illustrate strong contrasts between the marine and terrestrial sediments. Above ~375 °C, the marine sediments exhibit large increases in intensity, apparently due to oxidation of iron sulfides.

unconformities. On the southern flank, particularly in the more distal areas, sedimentation was finer grained (sandstone and siltstone are punctuated intermittently by conglomerate throughout the lower units), and most stratigraphic contacts appear to be conformable.

Given the distribution of facies and unconformities, more distal localities were chosen for magnetostratigraphic studies in finer grained, presumably more continuously deposited strata. The longest section (Oliana) is located on the southeast limb of the anticline (Figs. 3 and 5). It begins in the Igalada Formation, traverses both delta-front sandstone and strata laterally equivalent to the nearby Cardona evaporites, encompasses ~800 m of terrestrial strata, and termi-

nates in nearly continuous conglomeratic beds containing few, if any, fine-grained intercalations. The contact between the marine and terrestrial strata is demonstrably unconformable here because conglomerate 1 has been erosionally removed along the base of conglomerate 2 northeast of the section and is missing in the sampled strata (Figs. 3 and 5). Two other sections (Peramola I and II) are situated on the distal flank of the southwest-plunging nose of the anticline (Figs. 3 and 5). These sections are closer to the thrusts than is the Oliana section and contain higher proportions of coarse-grained strata. Consequently, suitable rock types for paleomagnetic studies are irregularly spaced. Both sections cross a distinctive unconformity

that separates conglomerates 1 and 2 (Fig. 5B) and can be used to correlate among all three sections.

Approximately 100 sampling sites were placed within these three sections. Sites were initially spaced at ~15-m stratigraphic intervals in the marine facies and at every 20 to 40 m in the fluvial sequence. During subsequent traverses, additional sites were placed in order to fill gaps where poor results had been previously obtained and to try to confirm magnetozones that were represented by fewer than three sites. At each site, 3 or 4 oriented specimens were collected. Paired specimens of representative rock types from these traverses were subjected to step-wise thermal demagnetization up to 600 °C

in order to characterize the magnetic behavior and to determine the optimal demagnetization procedures for the remaining samples.

The results from these pilot studies indicate two contrasting types of magnetic behavior for the marine and terrestrial strata. Often some component of the modern magnetic field is reflected by the initial *in situ* directions (Fig. 6). As much as 70% of the initial remanence, apparently comprising a viscous component and sometimes goethite, is lost during heating up to 250 °C. The characteristic remanence is typically revealed between 250 and 350 °C, and by 350 ° in the marine specimens, 50%–90% of the remanence intensity observed at 250 °C has been lost. Many of the marine samples show large intensity increases and unstable directions above 350–400 °C. This appears to result from oxidation of a low Curie-temperature mineral during heating and is interpreted as a conversion of an Fe-sulfide (probably greigite) to magnetite. A strong increase in susceptibility (Fig. 7) accompanies this thermally induced change in mineralogy.

Because iron sulfides are likely to be post-depositional in origin, there is some question about whether they record the magnetic field near the time of deposition. Studies of Holocene marine sediments (Karlin, 1990; Leslie and others, 1990a, 1990b) indicate that dissolution of magnetite and growth of greigite often occurs near the depositional surface (0–40 cm). Almost ubiquitously, marine-sediment accumulation rates defined using biostratigraphic and magnetostratigraphic data in the central Pyrenean foreland during Eocene times (Caus, 1973; Powers, 1989) are considerably greater than 10 cm/kyr, suggesting that greigite could have formed within <5–10,000 yr of deposition. Karlin (1990) noted that, when a complex magnetic signal represents both detrital and authigenic magnetic carriers, the preserved remanence directions often integrate several thousand years of secular variation. Whereas such sediments are not well suited for detailed magnetic studies requiring time resolutions of <10⁴ yr, they can, nonetheless, provide reliable polarity data (Karlin, 1990).

Magnetizations due to iron sulfides tend to be weak and are not always stable through time. Unfortunately, due to the paucity of reversed sites within the sampled marls, it is not possible to demonstrate a convincing reversal test based on the Oliana data. In conjunction with magnetic results from lithologically similar marl in nearby areas (Powers, 1989; Burbank and others, unpub. data), however, we conclude that the early post-depositional remanence directions at Oliana are being recovered based on the following observations: (a) the magnetic data pass a

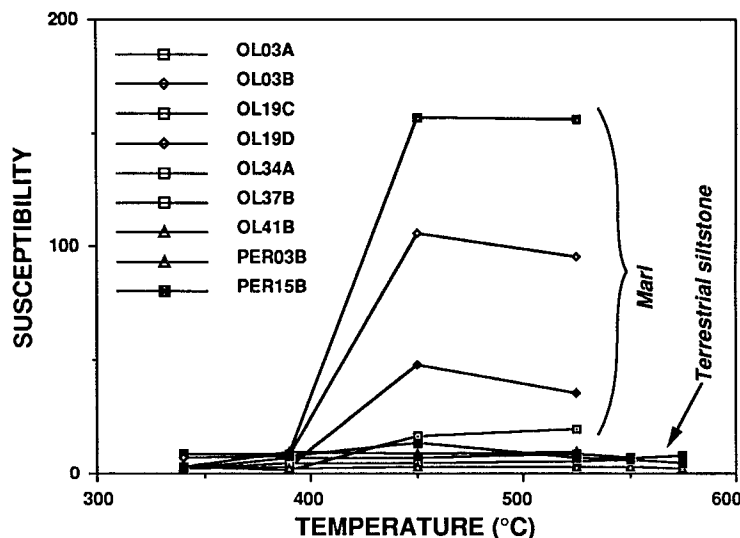


Figure 7. Susceptibility changes during thermal demagnetization. Large changes in susceptibility observed above 350 °C for many marine sediments mimic similar changes in intensity (Fig. 6). The observed susceptibility increases are interpreted to represent conversion of iron sulfides to magnetite during heating.

fold test (Table 1; McFadden and Jones, 1981), indicating that the magnetizations in the marls were acquired and stabilized prior to the folding that occurred shortly after deposition; (b) lithologically identical, superposed sites can show opposite polarities; and (c) in similar lithologies farther west in the SCU, laterally separated but demonstrably equivalent marine strata reveal matching patterns of reversals. Despite these contentions, the magnetic data are not of the highest quality, nor is the resulting magnetic zonation in the marls.

Whereas the fluvial strata also reveal their characteristic remanence directions between 250 and 350 °C, these directions and the magnetic susceptibility are generally stable up to ~550 °C (Figs. 6 and 7). Many of these strata are pink, tan, and red siltstones, and, in addition to magnetite as a primary remanence carrier, they indicate the likely presence of some authigenic hematite, as suggested by the remanence that remains above 580 °C (Fig. 6).

Because the directions interpreted to represent characteristic remanences were revealed for both marine and terrestrial samples at temperatures above ~240 °C, all of the remaining specimens were thermally demagnetized at 250, 280, 310, and 340 °C. A characteristic remanence direction was defined for each specimen based on these successive measurements. The validity of the specimen directions was further assessed using Fisher (1953) statistics on the multiple specimens at each temperature level at each site. Sites were then classified as “Class I,” if Fisher $k \geq 10$ (implying that these directions were non-random at >95% confidence level; Irving, 1964); “Class II,” when the polarity of the site was unambiguous, but $k \leq 10$; and “Class III,” when no reliable polarity could be determined for a site. The mean site directions, calculated using the 280–310 °C data, were used to determine a paleolatitude for the virtual geomagnetic pole (VGP) which in turn formed the basis for classifying sites as of either normal or reversed polar-

TABLE 1. FISHER STATISTICS ON MAGNETIC DATA

Section	Polarity	Number	<i>In situ</i>				Bedding corrected*			
			k	α_{95} (°)	Dec. (°)	Inc. (°)	k	α_{95} (°)	Dec. (°)	Inc. (°)
Oliana (all sites)	N	118	6.0	4.9	340.7	31.1	8.7	4.9	8.2	60.2
	R	58	6.3	8.6	155.8	18.0	7.0	8.2	164.5	-29.6
Oliana (marls)	N	81	6.8	6.6	332.6	34.8	11.3	4.9	357.3	62.2
Peramola I and II	N	24	8.6	12.2	340.0	21.7	4.1	20.4	345.8	20.4
	R	20	10.9	9.6	143.4	20.0	7.0	12.9	150.0	-27.5

k = Fisher (1953) k. α_{95} = 95% confidence interval on mean.
*Restored to horizontal attitude assuming nonplunging, cylindrical folds.

ity. An α_{95} -error envelope was calculated on the VGP latitude to provide an additional indication of the reliability of each site. Following demagnetization, some Class I and II sites exhibited inclinations that were inconsistent with their apparent polarity, that is, positive inclinations for sites with southerly VGP's. This was particularly true in the red beds of the Peramola sections, where more than 25% of the sites displayed this behavior. Such sites were not included in the magnetic polarity stratigraphy (MPS). They probably either represent transitional polarities or specimens for which a secondary overprint was not successfully removed.

Analysis of the magnetic data with respect to fold tests and VGP's is further complicated, because the sections are located along the flanks of a doubly plunging structure, the Peramola sections are located on a secondary plunging fold above a back thrust, and the anticlinal folding itself is not concentric. Given the available data, it is not possible at present to determine the plunge axis that would be appropriate for each part of each section. Consequently, reliable restoration of beds and magnetic directions to their pre-folding orientation is not readily accomplished (Chan, 1988), and apparent rotations revealed by the magnetic data should be evaluated in this context.

At present, the middle Cenozoic time scale is undergoing considerable revision (for example, Montanari and others, 1988; McIntosh, 1988; Berggren and Kent, 1989). Although we utilize the time scale of Berggren and others (1985) for our correlations, it is likely that all of the late Eocene to early Oligocene ages will be decreased by 2–4 m.y. Fortunately, the magnetic data cited here can be readily adjusted to accommodate these changes, and, because the early Eocene ages are also likely to be revised younger, the rates calculated here will not be strongly affected.

Following incremental decompaction (Sclater and Christie, 1980), tectonic subsidence was calculated using a force-balance approach, rather than the algorithm that is typically applied to wholly marine basins (see, for example, Sclater and Christie, 1980; Guidish and others, 1985). We assumed a force balance with local isostatic compensation at the beginning and end of each step of deposition, such that, at the end of each step, the difference between the isostatically predicted position of the base of the section and the modeled, decompacted position was attributed to tectonic loading. The summation of the incremental tectonic loads yielded the total tectonically driven subsidence. This approach can be applied equally to marine and terrestrial sediments, and it appears to improve the reliability of the estimate of tectonic subsidence.

RESULTS

Structural and Stratigraphic Results

Mapping (Vergés and Muñoz, 1990; and the present study) indicates that the eastern margin of the SCU is not a simple oblique-slip fault, but consists of two, related structural zones: an oblique imbricate system of thrust faults involving Mesozoic and lower Tertiary strata and a large, doubly plunging anticline in the Eocene strata of the footwall (Fig. 3). Well-exposed, crosscutting relationships between thrusts and syntectonic strata permit a clear reconstruction of the overall pattern of thrusting and growth of the anticline (Vergés and Muñoz, 1990). Strata that overlie thrust tips or that are either cut or deformed by thrusts indicate that both piggyback and hindward-imbricating thrusts are represented here: thus, two coeval, but contrasting styles of thrusting can be delineated.

Prior to the initiation of deformation, the Bartonian–lower Priabonian Igualeada marls accumulated across this region. During the latter part of marl deposition, a fan delta prograded across the northern portion of the study area. The final stages of fan-delta deposition were coeval with evaporitic deposition (Cardona) farther to the south. As shown by crosscutting relationships, the subsequently developed thrusts northwest of the Oliana anticline formed by hindward imbrication (Vergés and Muñoz, 1990). Hence, the oldest thrust is the southeastern-most Sierras Marginales thrust (Fig. 3), and the youngest thrust is the Montsec thrust.

Despite lithologic similarities among the hanging-wall strata of these thrust sheets, four distinct terrestrial conglomeratic packages can be delineated with respect to different episodes of break-back thrusting (Fig. 3). The crosscutting relationships between thrusts and syntectonic strata that serve to define these packages are best exposed along the northeastern exposures of the Sierras Marginales and Montsec thrusts (Fig. 3) where clear unconformities separate each of the conglomeratic units. Several of these units can be traced laterally around the northeastern and southwestern ends of the Oliana anticline and into the thicker stratigraphic sequence preserved along its southeast limb. As these contacts between the conglomeratic units are traced laterally toward more distal regions, they become increasingly conformable (with the exception of conglomerates 1 and 2, as described below), and distinctions among the stratal packets become less marked, such that a stratigraphic uncertainty of ~50 m should be attached to their mapped location. Deposition of conglomerate 1 largely preceded the initial thrusting event recorded in the Oliana area (Fig.

4C). In proximal positions, conglomerate 1 is cut by the outermost Sierras Marginales thrust, whereas in some more distal locations, its upper strata are deformed and/or eroded prior to deposition of conglomerate 2 (Fig. 5B). Although this initial thrust is “in sequence” (piggyback thrusting), it defines the southern limit of the hindward-imbricating stack of thrusts, as described below.

Mapping along the outermost Sierras Marginales thrust reveals that, whereas it truncates conglomerate 1, it is overlain unconformably by conglomerate 2 near the limits of its southern and northern exposures (Fig. 3). In the northern portion of the map area, a syntectonic progressive unconformity is developed within conglomerate 2 adjacent to a younger break-back thrust (Sierras Marginales II) that later truncated this conglomerate. In the direction of the hinterland, conglomerate 3, in turn, overlies the Sierra Marginales II thrust sheet and is itself folded into a footwall syncline by the Montsec thrust. This thrust not only cuts conglomerate 3, but its hanging wall was also the source of a large block (>200 m per side) that is preserved in the axis of the footwall syncline. Although strata equivalent to conglomerate 3 are undoubtedly present in the southwestern portion of the map area, they could not be unequivocally identified due to erosion of proximal portions of this unit. The final synorogenic conglomeratic package in the Oliana area, conglomerate 4, overlies the Montsec thrust (Fig. 3). In a few places, conglomerate 4 exhibits small amounts of local deformation above the buried thrust tip, but, in general, it defines the end of the hindward-imbricating thrust sequence.

As interpreted on the basis of field data, seismic lines, and well data, a contrasting style of deformation is represented by the growth of the Oliana anticline (Vergés and Muñoz, 1990). The subhorizontal Cardona evaporite underlies the anticline and indicates that it is allochthonous. In the anticlinal core, the Oliana well penetrated more than 2,300 m of Igualeada marls without encountering the evaporites. This is at least three times the documented stratigraphic thickness drilled in the Basella well (Fig. 4A). Due to the folding of the marls and their seismically defined thickening to the north, only two structural units are interpreted to have been superimposed in the core of the anticline (Fig. 4A). The absence of the Cardona evaporites in the drill hole, despite being present south and north of the study area, suggests that the anticline corresponds to a forward-dipping duplex (Vergés and Muñoz, 1990). Along the southeastern margin of the duplex, a back thrust separates conglomerate 1 from the underlying marls. This thrust and its hanging-wall anticline (Fig. 3) formed during

translation of the duplex across the footwall ramp. The duplex developed near the presently preserved northern margin of the Cardona evaporites which served as the detachment level. In contrast to, and in the context of, the Montsec and Sierras Marginales thrust, the Oliana duplex formed in a piggyback thrusting sequence.

Stratigraphic evidence indicates that the growth of the Oliana duplex was coeval with at least some parts of the break-back thrusting sequence. First, paleocurrents in the conglomerates northwest of the duplex (Oliana anticline) suggest flow primarily to the southwest, parallel to both the thrust and anticline traces. This stands in contrast to the transverse transport found associated with most proximal fan systems (for example, Marzo and Anadon, 1988; Bull, 1964). These fans appear, in part, to have poured into a structural moat that channeled flow along the northwest margin of the anticline against which conglomerates 2 and 3 pinch out locally. Second, on the southeast flank of the anticline and within the continental sediments, there is a low-energy, partly lacustrine succession. This sequence grades laterally both to the northeast and southwest into coarse conglomerates and suggests a protected environment in the lee of a structure that effectively diverted energetic flow around its flanks. This situation is similar to low-energy, inter-fan regions reconstructed along the northern margin of the Ebro basin (Hirst and Nichols, 1986). Third, the increasing truncation of conglomerate 1 by conglomerate 2 on the distal southeast flank of the Oliana structure (Figs. 3 and 5) suggests that it was growing during or just after deposition of conglomerate 1. Fourth, near the northeast nose of the anticline, stratal geometries within conglomerate 2 fan toward the southwest and pinch in the opposite direction above the unconformity. This suggests continued growth of the duplex during deposition of these conglomerates. Finally, at the widest part of the duplex along the Segre River, the preserved thickness of the conglomerates is at a minimum, implying continued deformation and some erosional truncation within this particular zone.

Balanced and Restored Cross Sections

A balanced cross section was constructed along a north-south transect, parallel to the thrust transport direction and across the zone of the Segre oblique ramps (Fig. 4). It is pinned in the south by the Sanajúa drill hole that penetrated the basement. Additional drill-hole data and nearby seismic sections help to define the subsurface structural geometries. The position of the footwall ramp of the autochthonous Eocene sediments is interpreted on the basis of the

northern, seismically defined extent of the flat-lying Cardona evaporites, changes in the dip angles within the Montsec thrust sheet (Fig. 4A), and well data.

Most of the shortening interpreted in the section is due to the displacement of the Mesozoic cover units (Sierras Marginales and Montsec) over allochthonous Eocene strata which form the Oliana duplex and to the displacement of this duplex structure above the décollement within the Cardona evaporites (Vergés and Muñoz, 1990). Both the large displacement involving the Igualada and Cardona Formations and the absence of south-vergent thrusts cutting either the surface of the anticline or the conglomeratic units south of it appear to be due to the efficacy of the Cardona detachment surface. This detachment surface continues southward into the foreland basin, where deformation of the hanging wall creates the southernmost structures in the Pyrenean fold-and-thrust belt (Vergés and others, 1991).

Two partially restored cross sections have been constructed (Figs. 4B and 4C). The older reconstruction indicates geometric relationships at the time of deposition of conglomerate 1 (Fig. 4C), whereas the younger restoration is contemporaneous with deposition of conglomerate 4 (Fig. 4B). The older restoration shows the position of the southward-prograding fan delta that crops out extensively in the northern flank of the Oliana anticline. The end of the fan-delta deposition corresponds to the closure of the marine basin and deposition of the early Priabonian Cardona evaporite, the top of which formed an extensive, subhorizontal surface. At this time, northern thrusts sheets, comprising Mesozoic to lower Eocene strata (the latter largely eroded in the present transverse), constituted the hinterland relief of the basin. Conglomerate 1, deposited across both this relief and the adjacent foreland strata, was subsequently deformed by the Sierras Marginales emergent imbricate fan of thrusts (Fig. 4C).

The second partially restored cross section corresponds in time with the base of conglomerate 4, which was deposited unconformably across the foreland strata, the growing duplex, and the break-back imbricate stack. Stratigraphic relationships permit the geometry of deformation, particularly the growth of the duplex and the amount of southward translation along the Cardona detachment, to be clearly delimited at the initiation of deposition of unit 4. At present, in the southern limb of the Oliana anticline, the basal contact of unit 4 is folded, whereas in the northern limb, it is flat lying and at a higher altitude. The altitudinal difference between the basal contact of unit 4 south of the anticline (where beds are again flat lying in the axis of a

syncline) and north of it corresponds to the height of the autochthonous footwall ramp. This geometry implies that unit 4 was deposited unconformably over the duplex and the break-back imbricates before the northern limb of the Oliana anticline climbed over the footwall ramp and consequently before most of the southward displacement of the studied structures across the detachment level took place (Fig. 4). The present geometry of the balanced cross section (Fig. 4A) is probably little altered since the end of early Oligocene time, when the youngest strata along this traverse (Sáez, 1987) were folded in the foreland fold-and-thrust belt.

On the basis of the balanced sections, minimum amounts of shortening can be calculated for three deformed zones: the Sierras Marginales imbricate fan and the Montsec thrust, the Oliana duplex, and the subsequent translation above the detachment south of the duplex. Shortening along the Sierras Marginales to Montsec thrusts (Figs. 3 and 4) amounts to at least 7.5 km. This shortening can be partitioned as follows: Sierras Marginales I (southernmost, floor thrust): 3.75 km; Sierras Marginales II (break-back sequence): 0.67 km; Montsec thrust: 2.15 km; and inversion of a previous Late Cretaceous Montsec normal fault (interpreted by the difference in thickness and facies between the footwall and the hanging wall of the Montsec thrust): 1.0 km. All of these estimates are minima because we do not know the position of the cut-off of the Mesozoic strata in the hanging wall. The likely predeformational positions of the Mesozoic strata now located in the imbricate fan and the position of the branch lines (Vergés and Muñoz, 1990) indicate that shortening is likely to have been considerably more than that calculated here. Regardless of any additional shortening, however, the deformation cited here represents syndepositional contraction that we can temporally constrain.

The shortening that resulted in the growth of the Oliana duplex is calculated to be 9.1 km. Whereas most of the duplex growth was coeval with the break-back thrusting, this terminated as extensive southward translation along the Cardona detachment commenced. The total amount of shortening along the cross section amounts to a minimum of 28.7 km, of which 16.7 km is attributed to break-back thrusting and duplex growth prior to deposition of conglomerate 4, whereas 12 km is assigned to subsequent southward translation.

Magnetic Results

The Oliana magnetic section (Fig. 5A) encompasses the upper 400 m of the marine sequence, all of conglomerates 2 and 3, and the

basal part of conglomerate 4, whereas the two Peramola sections (Figs. 5B) cover portions of conglomerates 1 and 2. The quality and reliability of the magnetic results vary significantly among the three sections. For the Oliana section, 61%, 14%, and 25% of the sites yielded Class I, II, and III data, respectively. The Peramola sections yielded 48%, 15%, and 37% Class I, II, and III sites, respectively. Nearly half of the statistically defined Class I sites in the Peramola sections, however, exhibited inclinations inconsistent with their calculated polarities (for example, positive inclinations with southerly declinations) and were discarded. Consequently, the MPS's here are more schematic and less reliable than in the Oliana section.

Twelve magnetozones are defined within the Oliana MPS (Fig. 8), most of which contain two or more sites. The two reversed magnetozones in the marls, however, are based on single Class II sites, and, despite further sampling, no additional reversed sites were located here. These magnetozones are, therefore, not well documented. Given the late Bartonian/early Priabonian age of the Igualada marls in the study area (Caus, 1973), magnetozones N1–N3 must correlate with some portion of chron 17 and possibly chron 18 (Aubry, 1985; Berggren and others, 1985; Fig. 9). The uncertainties respecting the validity of magnetozones R1 and R2 (Fig. 8) affect only the inferred age and correlation of the basal part of the studied section. Given the reversal pattern of the Eocene-Oligocene magnetic polarity time scale (MPTS, Berggren and others, 1985) and the Priabonian to early Rupelian age of the terrestrial conglomerates (Sáez, 1987), magnetozones N3–R6 can be correlated most reasonably with chrons 16N to 13R (Fig. 9). This correlation implies that the unconformity at the base of conglomerate 2 represents ~1 m.y.

Based on the correlation shown here, the base of conglomerate 2 is dated at ~39.2 Ma, and the last normal magnetozones (N6) correlates with chron 15 (~37.5 Ma). The mean rate of subsidence during this interval of terrestrial deposition averages ~20–25 cm/k.y. (Fig. 10). Because the upper 350 m of the sampled section is reversely magnetized, it appears to lie below chron 13N, and its top is estimated to date from ~36 Ma (Fig. 9). This correlation requires a slight acceleration of the subsidence rate during deposition of conglomerate 3 (Fig. 10).

It is, perhaps, surprising that the subsidence rate was lower during thrusting than prior to it (Fig. 10), at a time when geophysically based models for typical foreland basins would suggest enhanced subsidence should occur in response to thrust loading (Flemings and Jordan, 1989). Although the more rapid subsidence rates during

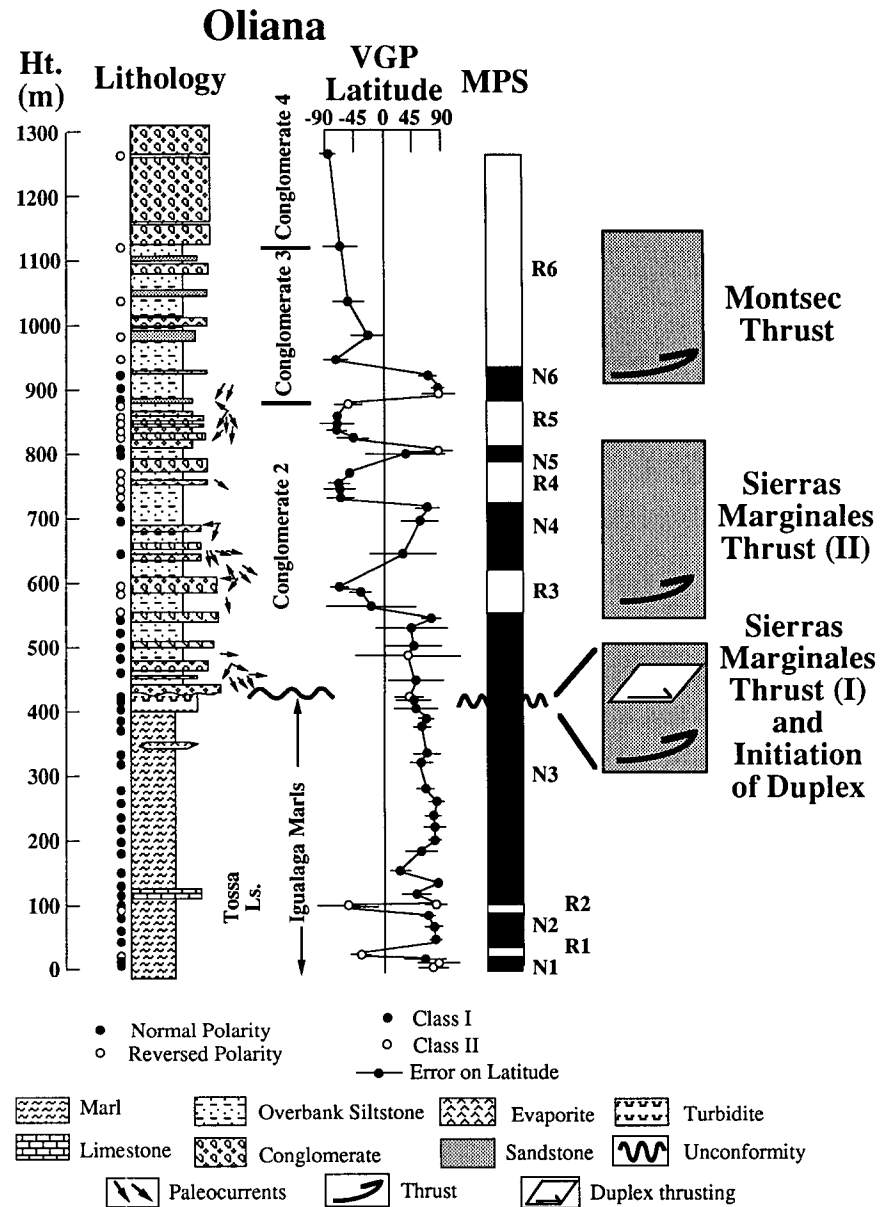


Figure 8. Magnetic polarity stratigraphy and simplified lithostratigraphy for the Oliana section (A) and for the Peramola I and II sections (B). The stratigraphic range of lithologic units referred to in the text is delineated. α_{95} -confidence intervals are plotted for each magnetic site. The boxes enclosing thrust symbols indicate the interval during which a specific thrust was active. For site and section locations, see Figures 3 and 5.

marl deposition (>35 cm/k.y.) could relate to undefined thrust loads emplaced farther to the north, the dramatic change in rates corresponds in time to the initial growth of the Oliana duplex. We infer that deposition of conglomerates 2–4 occurred above the roof thrust of the developing duplex and would have been affected by uplift during the ramping stages of duplex growth. The calculated decrease in the total amount of tectonically driven subsidence between the end of marl deposition and the begin-

ning of conglomerate 2 (Fig. 10) reinforces the concept of duplex growth and tectonic uplift at this time.

Both of the Peramola sections straddle the unconformity between conglomerates 1 and 2 (Fig. 5B) and are quite short (<400 m thick). Consequently, their MPS's can be interpreted only in the context of the Oliana magnetic section, which constrains conglomerate 1 to be older than chron 16 and younger than the underlying marl (~40.0 Ma). This suggests that N1 in

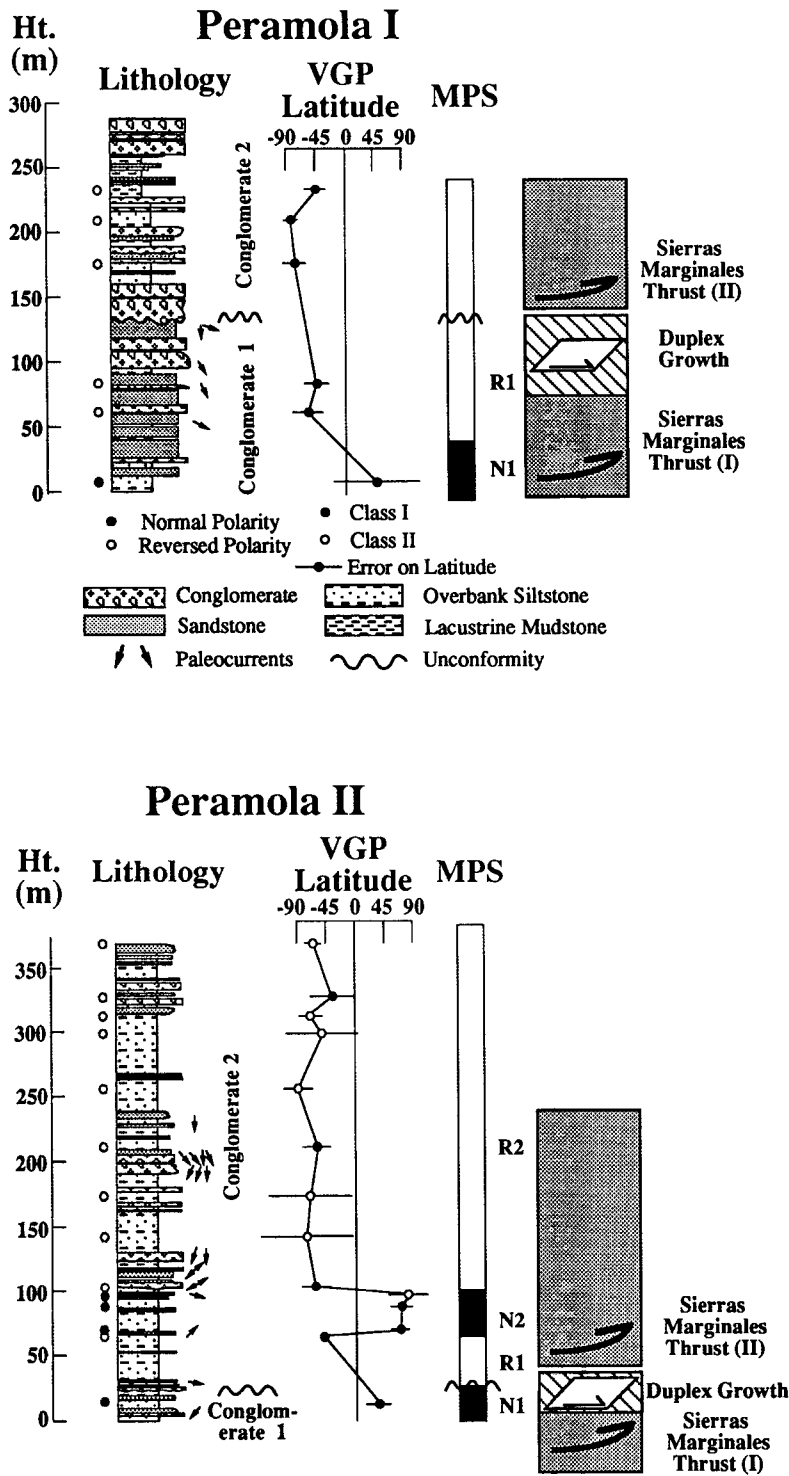


Figure 8. (Continued).

both Peramola sections should correspond with the top of chron 17 (Fig. 9). Due to the brevity of the Peramola sections, the correlation of conglomerate 2 with the MPTS is ambiguous, but the most logical interpretation suggests that it correlates with chron 15R and portions of chron 16. This interpretation requires the base of con-

glomerate 2 to be ~0.5 m.y. older in the Oliana section than in the Peramola sections. This would not be unexpected, given the tendency to preserve a more complete record in more distal sections, when proximal sections are being eroded during thrusting (Burbank and Reynolds, 1988). The age differences, however, also sug-

gest that deformation along the anticline was not uniform and that either the initial phases of duplex growth or back thrusting continued longer in the southwest than in the northeast. Although high rates of sediment accumulation for conglomerate 2 are required by this correlation (>60 cm/k.y.), such elevated rates might be anticipated immediately adjacent to thrusts, where both the sediment flux and subsidence should be highest. Moreover, considerable variability of short-term rates across distances of several kilometers is not unexpected (McRae, 1990).

Stereoplots and statistical analysis of the Class I data from Oliana and Peramola (Table 1 and Fig. 11) show that the bedding-corrected, normally and reversely magnetized sites are nearly antipodally disposed and that these data pass a fold test (McElhinny, 1964; McFadden and Jones, 1981). The observations that the mean *in situ* inclinations (4°–25°) are far shallower than the bedding-corrected inclinations (27°–60°) and that the *in situ* reversed inclinations are positive, rather than negative, reinforce the contention that the primary magnetization was acquired prior to folding. Although the data suggest the presence of a counterclockwise rotation, the difficulties in restoring beds in variably plunging structures (Chan, 1988) dictate that these apparent rotations should not be overinterpreted. The fact that the bedding-corrected, normal and reversed data from the Oliana section (Fig. 11A) are not completely antipodal may be due to the preponderance of normal sites in the basal third of the section. These strata require a different (but unknown) correction than do the overlying strata. The discrepancy between the mean declinations of the normal and reversed data may also be due to the incomplete removal of a normal overprint in some of the samples. Recent paleomagnetic studies of other Eocene strata (primarily sandstones) along the central portion and the SE margin of the Ebro basin (Parés and others, 1988) show a pervasive, high-temperature, normal-polarity remanence direction exhibiting ~20° of clockwise rotation. These Ebro basin sites fail both the reversal and fold tests and appear to carry a post-folding magnetization that may reside in fine-grained, authigenic hematite. A similar post-folding magnetization may bias some of the remanence directions determined for the Oliana data. Whereas this does not appear to interfere with the determination of polarity of sites, it may have deflected the mean declinations.

DISCUSSION

The structural and stratigraphic mapping in the Oliana-Peramola region reveals an unambiguous, hindward-imbricating system of thrusts

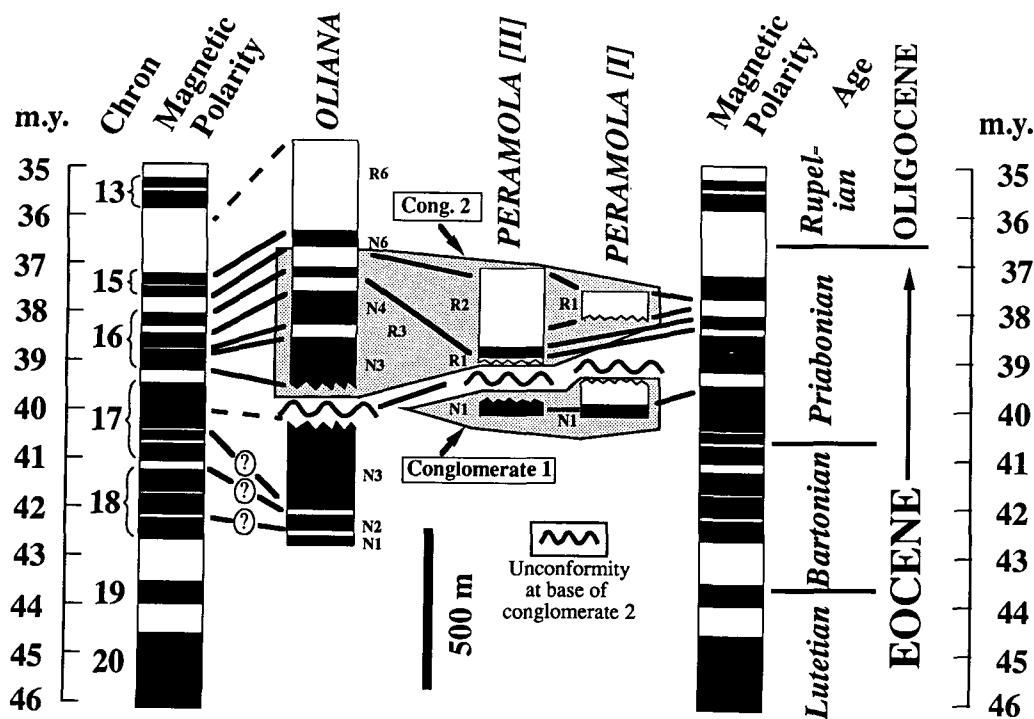


Figure 9. Correlation of the Oliana and the Peramola I and II magnetostratigraphies with the magnetic polarity time scale of Berggren and others (1985). The Bartonian/early Priabonian age (Caus, 1973) of N1–N3 in the Oliana section serves to tie the local MPS to the reversal time scale, although the precise correlation within chrons 17 and 18 is uncertain because not all of the reversed magnetozones were discovered. Stippled areas delineate the correlative conglomeratic strata among the sections. The age of the base of conglomerate 2 varies due to longer-lived deformation in the Peramola sections.

formed during an early phase of deformation (Vergés and Muñoz, 1990). Whereas the break-back system of thrusts represents a restricted amount of shortening (Fig. 4), it increased the structural relief and, consequently, the taper of the thrust wedge. Additional movement of the sole thrust of the Montsec and Sierras Marginales imbricates continued as deformation migrated farther into the foreland. Clear stratigraphic relationships indicate that growth of the Oliana duplex was concurrent with the development of the imbricate thrusts. The translation of the horses of the Oliana duplex across the footwall ramp (Fig. 4B) caused folding of both the previously emplaced thrusts and the coeval conglomeratic units. Consequently, thrust propagation both toward the foreland and the hinterland within a restricted geographical region can be unequivocally demonstrated to have occurred synchronously along the eastern margin of the SCU.

This region exhibits many similarities with the oblique ramp of the Pedraforca thrust sheet adjacent to the Ripoll basin in the eastern Pyrenees (Fig. 2). There, similarly unequivocal stratigraphic and structural evidence exists for a hindward-imbricating stack of thrusts that developed contemporaneously with a long-lived piggyback thrust (Martínez and others, 1988). As in the Oliana area, in the footwall of this imbricate stack, an anticline developed (Vilada anticline). In both areas, the eastern oblique ramp of a major thrust sheet is being examined, and a magnetically defined counterclockwise rotation

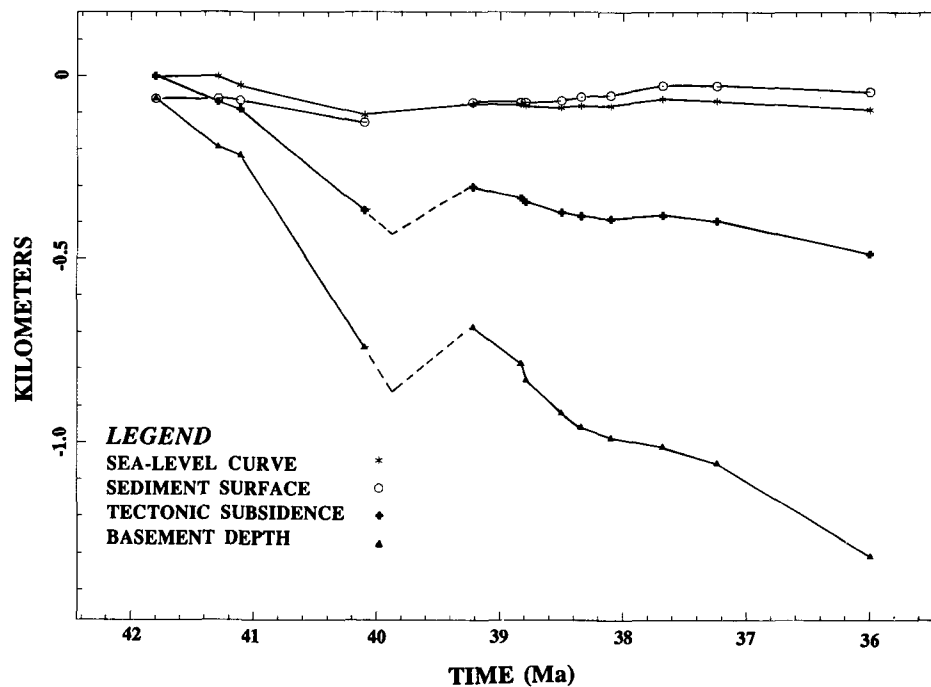


Figure 10. Geohistory curve for the Oliana section. Decompaction of sediments calculated using methods of Sclater and Christie (1980). The sea-level curve is from Haq and others (1987) and records departures from the initial sea-level position at ca. 42 Ma. The sediment surface indicates water depth for the marine sediments (>40 Ma) and the assumed height of the surface above sea level for the terrestrial sediments. The tectonic subsidence is calculated using a force-balance method (see text). Uncertainties in initial porosities, diagenetic history, past sea-level changes, and paleobathymetries suggest that an error envelope of ~10% should be attached to these subsidence calculations. The dashed lines indicate the approximate position of a hiatus in the record. The apparent uplift across this hiatus is interpreted to reflect initial growth of the Oliana duplex.

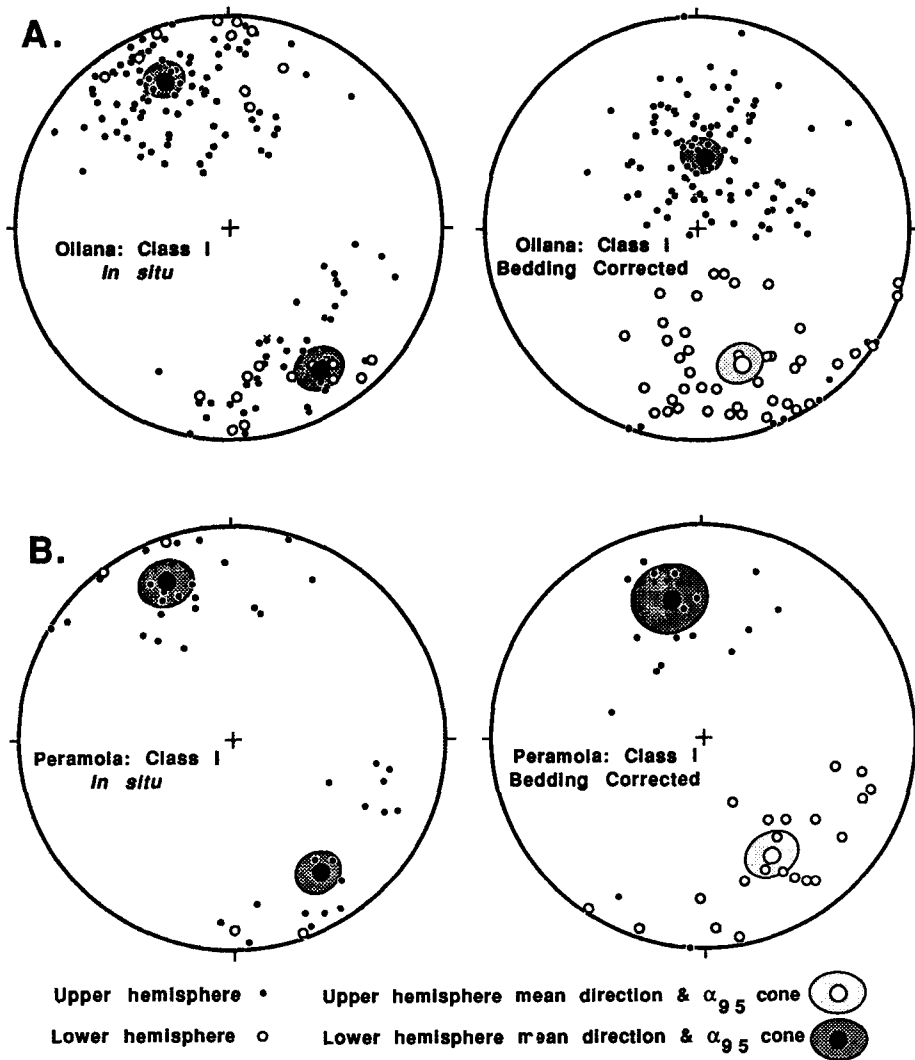


Figure 11. Equal-area stereonet plots of Class I magnetic data for Oliana (A) and Peramola (B) sections suggesting modest counterclockwise rotation, especially for the Peramola sections. Solid dots: lower-hemisphere data; open circles: upper-hemisphere data. The mean directions are calculated on the basis of those sites showing either northern or southern VGP latitudes in their bedding-corrected orientation. See text for discussion.

is observed in the basin immediately adjacent to the northeast-southwest-oriented structures (Burbank and Puigdefàbregas, 1985). This sense of rotation suggests that the thrust transport direction was oblique, rather than perpendicular, to the thrust traces. Such a transverse component of motion would be expected to generate a counterclockwise shear couple in the region east and south of the thrust tip.

When the chronologic data from the Oliana and Peramola magnetostratigraphic sections are combined with the structural data from the surrounding region, specific temporal limits can be placed on the deformational and depositional evolution of the eastern margin of the SCU (Fig. 12). Initial deformation in late Eocene time is represented by the upward-coarsening from

marls through fan-delta sandstones to conglomerates that developed as a thrust source area encroached on the northern margin of the study area. The deposition of the Cardona evaporites and the subsequent transition to terrestrial sedimentation in this region after 40.0 Ma appear to be coeval with a large, abrupt eustatic fall during early Priabonian times (Haq and others, 1987) and may in part be a response to this base-level change. Whereas the earliest terrestrial conglomerates on the southeast limb of the anticline were eroded in the vicinity of the Oliana section during early duplex development, they are preserved near the southwest-plunging nose of the structure (Fig. 3), where they were sampled by both Peramola sections. The magnetic data from these sections suggest that the basal portion of

conglomerate 1 dates from ~39.8 Ma. Conglomerate 2 is as old as 39.2 Ma in the distal areas (Oliana section), whereas in more proximal localities (where the effects of continuing deformation were more pronounced), its base dates from <39 Ma. This conglomerate contains a progressive unconformity in its proximal part and indicates continued motion on the northern strands of the Sierras Marginales thrust (Fig. 3). Although the precise correlation of conglomerate 3 from its proximal to more distal outcrops is somewhat tenuous due to incomplete exposure, this unit appears to span ~37.7–36.4 Ma. The termination of motion of the Montsec thrust, as represented by the generally undeformed, overlapping contact of conglomerate 4 across the thrust, can be dated at ~36.2 Ma. Given these chronologic data regarding individual thrusts, the entire imbricate package of thrusts can be shown to have developed over an interval of ~3.6 m.y. at a mean, minimum shortening rate of ~2.1 mm/yr.

The initiation of growth of the duplex can be inferred from the erosional truncation of conglomerate 1 in a “distal” position, that is, on the southeast limb of the anticline. The duration of erosion during initial duplex development extends from as old as 39.8 Ma until at least 39.3 Ma (the base of conglomerate 2 in the Oliana section). A second phase of syndepositional growth of the duplex is dated at ~39.2–38.0 Ma, as inferred from the progressive pinching of strata within conglomerate 2 both northwest and southeast of the anticline. The major phase of shortening within the duplex is inferred to have been completed before the initial deposition of conglomerate 4 (Fig. 4B). Because the folding and uplift of the basal contact of conglomerate 4 on the northwest limb of the Oliana anticline can be interpreted to have resulted from the translation of the duplex across the footwall ramp, the age of conglomerate 4 (~36.2 Ma at its base) places an upper limit on the timing of duplex growth. Given the 9 km of shortening calculated for the duplex itself (Fig. 4B), the mean shortening rate can be estimated as at least 2.5 mm/yr. Consequently, the total shortening rate across the deformed zone (thrust stack and duplex) is ~4.6 mm/yr during this 4-m.y.-long interval that encompasses much of Priabonian and the earliest part of Rupelian times.

The upper parts of conglomerate 4 could not be directly dated because the continuous, coarse-grained strata prevented further magnetic sampling. If the sediment-accumulation rates determined for the upper portion of the dated Oliana section (Fig. 10) are extrapolated to the top of the folded units, they would date from ~34.5 Ma. We take this estimated age to represent the termination of translation of the duplex across

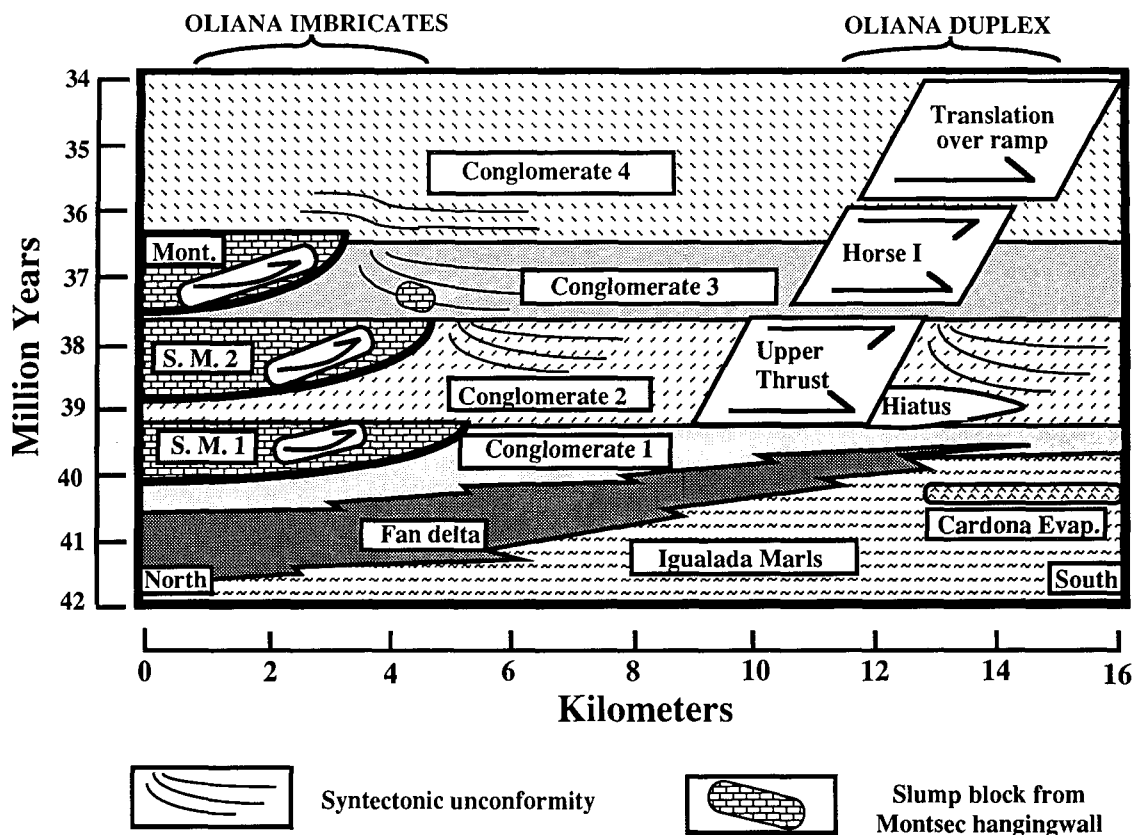


Figure 12. Time-distance summary of thrusting, duplex growth, and related deposition. Four dated conglomeratic packages are displayed with respect to the thrusts that they overlap or by which they are cut. The age of the boundary between conglomerates 2 and 3 is not tightly constrained. Although the overall timing of the duplex development is well defined, the specific sequencing and timing of motion on individual horses is speculative. S.M. = Sierras Marginales; Mont. = Montsec.

the ramp. Given ~3–5 km required to complete this translation (Fig. 4B), a shortening rate of 2.5–4 mm/yr can be estimated for this interval.

This new chronology from the Oliana region serves to constrain more precisely the development of two of the major thrust systems in the SCU (Fig. 2). The oblique margin of the Sierras Marginales thrust system was active in the Oliana area from ~40.0 to ~37.5 Ma. This deformation is inferred to be both synchronous with, and directly related to, the earliest major phase of thrusting along the southern deformed margin of the SCU. Later stages of emplacement of the SCU and additional Oligocene deformation in the Sierras Marginales is probably represented near Oliana both by continued growth of the duplex and by later southward translation along the detachment that underlies both the thrust stack and the duplex (Fig. 3).

Although bounded on the west by the north-south Boltaña anticline, the Sierras Marginales appear to be cartographically related to the Sier-

ras Exteriores, which delimit the southern margin of the Guarga thrust sheet 100–200 km to the west of the study area (Fig. 1). When compared with similar magnetic chronologies for deformation developed in the Sierras Exteriores (Hogan and others, 1988; Jolley and Hogan, 1989), the dates from the Sierras Marginales indicate that emplacement of the southern thrust sheets of the SCU began ~4 m.y. prior to the initiation of major thrusting in the Sierras Exteriores.

Whereas the Montsec thrust was clearly active in early Eocene time (Mutti and others, 1985; Powers, 1989), reactivation of this thrust along the northern margin of the Ager basin is inferred to correlate with Montsec thrusting in the Oliana area, that is, 37.5–36.2 Ma. It is interesting to note that renewal of activity on the Montsec thrust in the Ager area thus occurred ~16 m.y. after the initial phase of motion ceased along this fault in the early Eocene. It also appears that the most important phase of shorten-

ing along the northern limit of the Ager basin was the latest Eocene–Oligocene interval of thrusting, as defined in the Oliana area.

CONCLUSIONS

The synthesis of detailed chronologic, structural, and stratigraphic data from the southern Pyrenees provides new insights upon the timing and styles of deformation within a thrust foreland, as well as upon the rates of major deformational and depositional events in this particular orogen. Geologic mapping along the oblique ramp of the South-Central Unit in the Oliana region serves to define two contrasting styles of shortening that occurred both coevally and immediately adjacent to each other. Crosscutting stratigraphic and structural relationships clearly show that a hindward-imbricating stack of thrusts developed along the Segre oblique ramp. While these thrusts were active, piggyback thrusting led to the development of a neighbor-

ing duplex to the southeast of the thrust stack. Balanced sections suggest that a minimum of ~16.7 km of shortening is represented by the imbricate stack and the duplex.

Magnetostratigraphic dating indicates that marine sedimentation continued in this area until ~40.0 Ma, after which conglomerate 1, derived from hinterland sources, transgressed across the northwestern part of the study area. Motion along the Sierras Marginales thrust commenced ca. 39.8 Ma, and during the next 3.6 m.y., the imbricate stack developed at a mean shortening rate of ~2.1 mm/yr. Growth of the Oliana duplex (at a mean rate of ~2.5 mm/yr) occurred during this same interval, such that the net shortening rate was ~4.6 mm/yr. Translation at comparable rates of the duplex across the footwall ramp was likely to have been completed by ~34.5 Ma. These rate data indicate that, although the deformation was partitioned into distinctively different styles (hindward imbrication, duplex growth, and translation on a décollement) and may also have occurred in discrete pulses along individual thrusts, the mean rate of shortening remained steady throughout the 5-m.y.-long interval.

Thrusts within the imbricate stack at Oliana appear to be strands of the Sierras Marginales and Montsec thrust systems that define two major east-west zones of deformation within the SCU. Consequently, the locally determined chronologic records can be utilized to delimit important intervals of large-scale shortening in the South Pyrenean foreland. The magnetostratigraphic dates from the Oliana region indicate that the initial phase of shortening in the Sierras Marginales extended from 39.8 to 37.5 Ma, whereas the final phase of motion on the Montsec thrust commenced at ~37.5 Ma and terminated at ~36 Ma. The thrust-wedge model (Davis and others, 1983) predicts that, in order to maintain a critical taper, deformation must occur within the wedge, as well as at its leading edge. The out-of-sequence character defined by this thrust chronology for the SCU supports this prediction.

ACKNOWLEDGMENTS

This research was partially supported by National Science Foundation grants EAR-8517482 and EAR 8816181. In addition, acknowledgment is made to the donors of the Petroleum Research Fund, administered by the American Chemical Society (ACS-PRF 20591) and PRF 17625) for their generous support. Discussions

with Cai Puigdefàbregas and Steve Lund have greatly enhanced this work. The careful work of Karen Young in the USC paleomagnetism lab is gratefully acknowledged. Stereonet programs were provided by Rick Allmendinger. Paleobathymetric estimates provided by J. Serra-Kiel and E. Caus were helpful in our subsidence calculations. Thoughtful reviews by Teresa Jordan and David Anastasio greatly improved this manuscript.

REFERENCES CITED

- Aubry, M. P., 1985, Northwestern European Paleogene magnetostratigraphy, biostratigraphy, and paleogeography: Calcareous nanofossil evidence: *Geology*, v. 13, p. 198-202.
- Bally, A. W., Gordy, P. L., and Stewart, G. A., 1966, Structure, seismic data, and orogenic evolution of southern Canadian Rockies: *Bulletin of Canadian Petroleum Geology*, v. 14, p. 337-381.
- Berggren, W. A., and Kent, D. V., 1989, Late Paleogene time-scale: An update: *Geological Society of America Abstracts with Programs*, v. 21, p. 86.
- Berggren, W. A., Kent, D. V., Flynn, J. J., and van Couvering, J. A., 1985, Cenozoic geochronology: *Geological Society of America Bulletin*, v. 96, p. 1407-1418.
- Boyer, S. E., and Elliott, D., 1982, Thrust systems: *American Association of Petroleum Geologists Bulletin*, v. 66, p. 1196-1230.
- Bull, W. B., 1964, Geomorphology of segmented alluvial fans in western Fresno County, California: *U.S. Geological Survey Professional Paper* 532-F.
- Burbank, D. W., and Puigdefàbregas, C., 1985, Chronologic investigations of the South Pyrenean basins: Preliminary magnetostratigraphic results from the Ripoll Basin: *International Association of Sedimentologists Sixth European Regional Meeting Abstracts and Poster Abstracts*, Lleida, Spain, p. 66-69.
- Burbank, D. W., and Reynolds, R. G. H., 1988, Stratigraphic keys to the timing of thrusting in terrestrial foreland basins: Applications to the northwestern Himalaya, in Kleinspehn, K. L., and Paola, C., eds., *New perspectives in basin analysis*: New York, Springer-Verlag, p. 331-351.
- Caus, E., 1973, Aportaciones al conocimiento del Eoceno del anticlinal de Oliana (Prov. de Lérida): *Acta Geológica Hispánica*, v. 8, p. 7-10.
- Chan, L. S., 1988, Apparent tectonic rotations, declination anomaly equations, and declination anomaly charts: *Journal of Geophysical Research*, v. 93, p. 12,151-12,158.
- Davis, D., Suppe, J., and Dahlen, F. A., 1983, Mechanics of fold-and-thrust belts and accretionary wedges: *Journal of Geophysical Research*, v. 88, p. 1153-1172.
- Dinarés, J., McClelland, E., and Santanach, P., 1991, Contrasting rotations within thrust sheets and kinematics of thrust-tectonics as derived from paleomagnetic data: An example from the southern Pyrenees, in McClay, K., ed., *Thrust tectonics*: Cambridge, Massachusetts, Unwin Hyman.
- ECORS Pyrenees team, 1988, The ECORS deep reflection seismic survey across the Pyrenees: *Nature*, v. 331, p. 508-511.
- Elliott, T., Graham, R. H., Ghibaudo, G., Apps, G., Evans, M., and Davies, A. H., 1985, A structural and sedimentological traverse through the Tertiary foreland basins of the External Alps of south-east France: *International Symposium on Foreland Basins. Excursion Guidebook*, p. 39-73.
- Fisher, R. A., 1953, Dispersion on a sphere: *Royal Society of London Proceedings*, v. A217, p. 295-305.
- Flemings, P. B., and Jordan, T. E., 1989, A synthetic stratigraphic model of foreland basin development: *Journal of Geophysical Research*, v. 94, p. 3851-3866.
- Guidish, T. M., Kendall, C. G., St. C., Lerche, I., Toth, D. J., and Yazab, R. F., 1985, Basin evaluation using burial history calculations: An overview: *American Association of Petroleum Geologists Bulletin*, v. 69, p. 92-105.
- Haq, B. U., Hardenbol, J., and Vail, P. R., 1987, Chronology of fluctuating sea levels since the Triassic: *Science*, v. 235, p. 1156-1167.
- Hirst, J.P.P., and Nichols, G. J., 1986, Thrust tectonic controls on Miocene alluvial distribution patterns, southern Pyrenees, in Allen, P. A., and Homewood, P., eds., *Foreland basins*: *International Association of Sedimentologists Special Publication 8*: London, England, Blackwell Scientific Publications, p. 247-258.
- Hogan, P. J., Burbank, D. W., and Puigdefàbregas, C., 1988, Magnetostratigraphic chronology of the sedimentologic and tectonic evolution of the Jaca Basin, southwestern Pyrenees, in Muñoz, J. A., Sanz, C., and Santanach, P., eds., *Symposium on the Geology of the Pyrenees and Betics*: Barcelona, Servei Geològic de Catalunya, p. 76.
- Irving, E., 1964, Paleomagnetism and its application to geological and geophysical problems: New York, Wiley, 399 p.
- Jolley, E. J., and Hogan, P. J., 1989, The Campodarbe Group of the Jaca basin, in Friend, P. F., Hirst, J.P.P., Hogan, P. J., Jolley, E. J., McElroy, R., Nichols, G. J., and Rodríguez Vidal, J., eds., *Pyrenean tectonic control of Oligo-Miocene river systems*, Huesca, Aragon, Spain, Fourth International Fluvial Conference Excursion Guidebook 4: Servei Geològic de Catalunya, p. 93-120.
- Jordan, T. E., Flemings, P. B., and Beers, J. A., 1988, Dating thrust-fault activity by use of foreland-basin strata, in Kleinspehn, K. L., and Paola, C., eds., *New perspectives in basin analysis*: New York, Springer-Verlag, p. 307-330.
- Karlin, R., 1990, Magnetite diagenesis in marine sediments from the Oregon continental margin: *Journal of Geophysical Research*, v. 95, p. 4405-4419.
- Leslie, B. W., Lund, S. P., and Hammond, D. E., 1990a, Rock magnetic evidence for the dissolution and authigenic growth of magnetic minerals within anoxic marine sediments of the California continental borderland: *Journal of Geophysical Research*, v. 95, p. 4437-4352.
- Leslie, B. W., Hammond, D. E., Berelson, W. M., and Lund, S. P., 1990b, Diagenesis in anoxic sediments from the California continental borderland and its influence on iron, sulfur, and magnetite behavior: *Journal of Geophysical Research*, v. 95, p. 4453-4470.
- Martínez, A., Vergés, J., and Muñoz, J. A., 1988, Secuencias de propagación del sistema de cabalgamientos de la terminación oriental del manto del Pedraforca y relación con los conglomerados sinorogénicos: *Acta Geológica Hispánica*, v. 23, p. 119-128.
- Marzo, M., and Anadon, P., 1988, Anatomy of a conglomerate fan-delta complex: The Eocene Montserrat conglomerate, Ebro basin, northeastern Spain, in Nemeq, W., and Steel, R. J., eds., *Fan deltas: Sedimentology and tectonic settings*: Glasgow, Scotland, Blackie and Son, p. 318-340.
- McElhinny, M. W., 1964, Statistical significance of the fold test in paleomagnetism: *Royal Astronomical Society Geophysical Journal*, v. 8, p. 328-340.
- McFadden, P. L., and Jones, D. L., 1981, The fold test in paleomagnetism: *Royal Astronomical Society Geophysical Journal*, v. 67, p. 53-58.
- McIntosh, W. C., 1988, Progress toward calibration of mid-Tertiary geomagnetic polarity history using high-precision ⁴⁰Ar-³⁹Ar geochronology of ignimbrite sequences in SW New Mexico: *Geological Society of America Abstracts with Programs*, v. 21, p. 65-66.
- McRae, L. E., 1990, Paleomagnetic isochrons, unsteadiness, and non-uniformity of sedimentation in Miocene fluvial strata of the Siwalik Group, northern Pakistan: *Journal of Geology*, v. 98, p. 433-456.
- Montanari, A., DePaulo, D. J., Alvarez, W., Drake, R., Curtis, G. H., Odín, G. S., Turrin, B., and Bice, D. M., 1989, Radio-isotopic calibration of the upper Eocene and Oligocene magnetic polarity and foraminiferal time scales in the northern Apennines of Italy: *Geological Society of America Abstracts with Programs*, v. 21, p. 178.
- Muñoz, J. A., 1991, Evolution of a continental collision: ECORS-Pyrenees crustal balanced cross-section, in McClay, K., ed., *Thrust tectonics*: Cambridge, Massachusetts, Unwin Hyman.
- Mutti, E., Rosell, J., Allen, G. P., Fonesse, F., and Sgavetti, M., 1985, The Eocene Baronia tide dominated delta-shelf system in the Ager Basin: *International Association of Sedimentologists 6th European Regional Meeting, Excursion Guidebook*, p. 579-600.
- Parés, J.-M., Banda, E., and Santanach, P., 1988, Paleomagnetic results from the southeastern margin of the Ebro Basin (NE Spain): *Physics of Earth and Planetary Interiors*, v. 52, p. 267-282.
- Platt, J. P., 1988, Dynamics of orogenic wedges and the uplift of high-pressure metamorphic rocks: *Geological Society of America Bulletin*, v. 97, p. 1037-1053.
- Powers, M. K., 1989, Magnetostratigraphy and rock magnetism of Eocene foreland basin sediments, Esera and Isabena valleys, Treppe-Graus Basin, southern Pyrenees, Spain [M.Sc. thesis]: Los Angeles, California, University of Southern California, 225 p.
- Puigdefàbregas, C., Collinson, J., Cuevas, J. L., Dreyer, T., Marzo, M., Mellere, D., Mercade, L., Muñoz, J. A., Nijman, W., and Vergés, J., 1989, Alluvial deposits of the successive foreland basin stages and their relation to the Pyrenean thrust sequence, in Marzo, M., and Puigdefàbregas, C., eds., *Fourth International Conference on Fluvial Sedimentology Guidebook*: Barcelona, Servei Geològic de Catalunya, 175 p.
- Roure, F., Choukroune, P., Berastegui, X., Muñoz, J. A., Villien, A., Matheron, P., Bareyt, M., Séguret, M., Cámara, P., and Deramond, J., 1989, ECORS deep seismic data and balanced cross sections: Geometric constraints on the evolution of the Pyrenees: *Tectonics*, v. 8, p. 41-50.
- Sáez, A., 1987, Estratigrafía y sedimentología de las formaciones lacustres del tránsito Eoceno-Oligoceno del NE de la cuenca del Ebro [Ph.D. dissertation]: Barcelona, Spain, University of Barcelona, 352 p.
- Séguret, M., 1972, Étude tectonique des nappes et séries décollées de la partie centrale du versant sud des Pyrénées: *Publication USTELA, Series Géologie et Structure*, no. 2, Montpellier, France.
- Sclater, J. G., and Christie, R. A. F., 1980, Continental stretching: An explanation of the post-mid-Cretaceous subsidence of the central North Sea Basin: *Journal of Geophysical Research*, v. 85, p. 711-739.
- Simó, A., 1985, Secuencias deposicionales del Cretácico superior de la Unidad del Montsec (Pirineo Central) [Ph.D. dissertation]: Barcelona, Spain, University of Barcelona, 326 p.
- Vergés, J., and Muñoz, J. A., 1990, Thrust sequences in the southern central Pyrenees: *Bulletin de la Société Géologique de France*, v. 8, p. 265-271.
- Vergés, J., Muñoz, J. A., and Martínez, A., 1991, South Pyrenean fold-and-thrust belt: Role of foreland evaporitic levels in thrust geometry, in McClay, K., ed., *Thrust tectonics*: Cambridge, Massachusetts, Unwin Hyman.